# HOKKAIDO UNIVERSITY

| | |
|---|---|
| Title | Enzymatic characteristics of d-mannose 2-epimerase, a new member of the acylglucosamine 2-epimerase superfamily |
| Author(s) | Saburi, Wataru; Sato, Suzuka; Hashiguchi, Saki; Muto, Hirohiko; Iizuka, Takahisa; Mori, Haruhide |
| Citation | Applied microbiology and biotechnology, 103(16), 6559-6570<br>https://doi.org/10.1007/s00253-019-09944-3 |
| Issue Date | 2019-08 |
| Doc URL | http://hdl.handle.net/2115/79027 |
| Rights | The final publication is available at link.springer.com |
| Type | article (author version) |
| File Information | 190520_ME.pdf |

1   **Enzymatic characteristics of D-mannose 2-epimerase, a new member of the acylglucosamine 2-**

2   **epimerase superfamily**

3

4

5   Wataru Saburi,[1,*] Suzuka Sato,[1] Saki Hashiguchi,[1] Hirohiko Muto,[1] Takahisa Iizuka,[2] and Haruhide

6   Mori[1,*]

7   [1]*Research Faculty of Agriculture, Hokkaido University, Kita 9, Nishi 9, Kita-ku, Sapporo 060-8589,*

8   *Japan*

9   [2]*Nihon Shokuhin Kako Co., Ltd., 30 Tajima, Fuji, Shizuoka 417-8530, Japan*

10

11   *Corresponding authors. Tel/Fax: +81-11-706-2508; E-mail: saburiw@chem.agr.hokudai.ac.jp (W.

12   Saburi). Tel/Fax: +81-11-706-2497; E-mail: hmori@chem.agr.hokudai.ac.jp (H. Mori).

13

14

15

16

17

18

19

20

21    **Abstract**

22        Carbohydrate epimerases and isomerases are essential for the metabolism and synthesis of

23    carbohydrates. In this study, *Runella slithyformis* Runsl_4512 and *Dyadobacter fermentans* Dfer_5652

24    were characterized from a cluster of uncharacterized proteins of the acylglucosamine 2-epimerase (AGE)

25    superfamily. These proteins catalyzed the intramolecular conversion of D-mannose to D-glucose, whereas

26    they did not act on β-(1→4)-mannobiose, *N*-acetyl-D-glucosamine, and D-fructose, which are substrates

27    of known AGE superfamily members. The $k_{cat}/K_m$ values of Runsl_4512 and Dfer_5652 for D-mannose

28    epimerization were 3.89 and 3.51 $min^{-1}mM^{-1}$, respectively. Monitoring the Runsl_4512 reaction through

29    $^1$H-NMR showed the formation of β-D-glucose and β-D-mannose from D-mannose and D-glucose,

30    respectively. In the reaction with β-D-glucose, β-D-mannose was produced at the initial stage of the

31    reaction, but not in the reaction with α-D-glucose. These results indicate that Runsl_4512 catalyzed the 2-

32    epimerization of the β-anomer substrate with a net retention of the anomeric configuration. Since $^2$H was

33    obviously detected at the 2-C position of D-mannose and D-glucose in the equilibrated reaction mixture

34    produced by Runsl_4512 in $^2H_2O$, this enzyme abstracts 2-H from the substrate and adds another proton

35    to the intermediate. This mechanism is in accordance with the mechanism proposed for the reactions of

36    other epimerases of the AGE superfamily, that is, AGE and cellobiose 2-epimerase. Upon reaction with

37    500 g/L D-glucose at 50°C and pH 8.0, Runsl_4512 and Dfer_5652 produced D-mannose with a 24.4 and

38    22.8% yield, respectively. These D-mannose yields are higher than those of other enzyme systems, and

39    ME acts as an efficient biocatalyst for producing D-mannose.

40    Keywords: D-mannose; epimerase; cellobiose 2-epimerase; acylglucosamine 2-epimerase; D-mannose

2

41    isomerase

42

43    **Introduction**

44        Carbohydrates are the most abundant organic compounds in nature; they have diverse structures due

45    to presence of various monosaccharide units, linkages, and degrees of polymerization. To metabolize

46    carbohydrates, organisms utilize several intra- and extracellular enzymes, such as glycoside hydrolases,

47    glycoside phosphorylases, and sugar isomerases/epimerases. Moreover, these metabolizing enzymes have

48    great potential for application in carbohydrate synthesis. As only few carbohydrate types, including

49    starch, sucrose, and lactose, are abundantly available, enzymatic conversion of abundant sugars to rare

50    sugars is required to utilize rare sugars as foodstuffs and drags.

51        Carbohydrate isomerases and epimerases catalyze the isomerization (conversion between aldose and

52    ketose) and epimerization (conversion between epimers) of carbohydrates, respectively. These enzymes

53    are essential in major carbohydrate metabolic pathways including glycolysis, oxidative/reductive pentose

54    phosphate pathways, and Leloir pathway, and provide suitable reactions for carbohydrate conversions.

55    For instance, isomerization of D-glucose to D-fructose by D-xylose isomerase (EC 5.3.1.5) is widely

56    applicable in the production of D-fructose-rich syrup (Bhosale et al. 1996). Furthermore, D-xylose

57    isomerase facilitates biofuel production from lignocellulosic biomass (Kuyper et al. 2004). Cellobiose 2-

58    epimerase (CE; EC 5.1.3.11) produces epilactose [β-D-galactopyranosyl-(1→4)-D-mannose] from lactose

59    via 2-epimerization of reducing end sugar residue (Ito et al. 2008; Saburi et al. 2010). This disaccharide

60    has a prebiotic property (Watanabe et al. 2008) and enhances mineral absorption (Nishimukai et al. 2008;

3

61     Suzuki et al. 2010a; Suzuki et al. 2010b) and energy expenditure in the skeletal muscle and brown

62     adipose tissues in order to avoid obesity (Murakami et al. 2015). D-Tagatose 3-epimerase (EC 5.1.3.31)

63     isomerizes D-fructose to produce D-psicose (Takeshita et al. 2000). D-Psicose is not metabolized by

64     humans (Iida et al. 2010) and exhibits antiobesity activity by increasing the energy expenditure (Ochiai et

65     al. 2013; Ochiai et al. 2014). UDP-galactose 4-epimerase (EC 5.1.3.2) is applied to the enzymatic

66     production of lacto-*N*-biose I [β-D-galactopyranosyl-(1→3)-*N*-acetyl-D-glucosamine], which is a part of

67     type I human milk oligosaccharide and has prebiotic property (Nishimoto et al. 2007; Kiyohara et al.

68     2009).

69        Acylglucosamine 2-epimerase (AGE) superfamily includes several carbohydrate epimerases and

70     isomerases: AGE (EC 5.1.3.8) (Itoh et al. 2000; Lee et al. 2007), CE (Saburi 2016), D-mannose isomerase

71     (MI; EC 5.3.1.7) (Kasumi et al. 2014; Saburi et al. 2018), and sulfoquinovose isomerase (SQI; EC

72     5.3.1.31) (Denger et al. 2014). These enzymes share an $(\alpha/\alpha)_6$-barrel folded catalytic domain (Itoh et al.

73     2000; Lee et al. 2007; Saburi et al. 2018; Fujiwara et al. 2013; Fujiwara et al. 2014; Itoh et al. 2008). Two

74     catalytic His residues on 8th and 12th α-helices of the catalytic domain and several residues for substrate

75     binding are completely conserved throughout the family. During epimerization of *N*-acetyl-D-

76     glucosamine and D-glucose residue of β-(1→4)-disaccharides by AGE and CE, respectively, catalytic His

77     on the 12th α-helix abstracts the axial proton from 2-C of the substrate as general base catalyst in order to

78     generate the *cis*-endiolate intermediate, and His on the 8th α-helix donates the proton to the intermediate

79     as general acid catalyst for producing the epimerized product (Lee et al. 2007; Fujiwara et al. 2014).

80     During isomerization of D-mannose to D-fructose by MI, His on the 8th α-helix mediates intramolecular

4

81    proton transfer between 1-C and 2-C (Itoh et al. 2008; Saburi et al. 2018).

82        In this study, a new carbohydrate epimerase, D-mannose 2-epimerase (ME), which can catalyze the

83    2-epimerization of D-glucose and D-mannose, was found via the functional analysis of the *Runella*

84    *slithyformis* Runsl_4512 and *Dyadobacter fermentans* Dfer_5652 proteins present in an uncharacterized

85    cluster of AGE superfamily proteins (Fig. 1). Enzymatic properties of these enzymes and the mechanism,

86    through which they produce D-mannose from D-glucose, are described.

87

88    **Materials and methods**

89    *Phylogenetic analysis of AGE superfamily proteins*

90        Multiple sequence alignment of AGE superfamily enzymes was conducted using MAFFT version 7

91    (Katoh et al. 2017), and a phylogenetic tree was prepared using all gap-free sites (69 amino acid

92    residues) through the neighbor joining method. The phylogenetic tree was visualized using a Figtree

93    program version 1.4.3 (http://tree.bio.ed.ac.uk/software/figtree/).

94

95    *Preparation of expression plasmids*

96        The genes, encoding Runsl_4512 and Dfer_5652 (Genbank numbers, AEI50834.1 and ACT96842.1)

97    were amplified from the genomic DNA via PCR using Primestar HS DNA polymerase (Takara Bio,

98    Kusatsu, Japan). The genomic DNA of *R. slithyformis* DSM19594 and *D. fermentans* ATCC700827 were

99    purchased from Deutsche Sammlung von Mikroorganismen und Zellkulturen (Braunschweig, Germany)

100    and the American Type Culture Collection (Manassas, VA, USA), respectively. The primer sequences are

101      listed in Table 1. Amplified PCR products were inserted into pET-23a vector (Novagen, Darmstadt,

102      Germany) via the restriction endonuclease sites: *Nde*I and *Xho*I sites for *Runsl_4512*, and *Eco*RI and *Xho*I

103      sites for *Dfer_5652*. The recombinant enzymes had extra eight residues, Leu-Glu-His-His-His-His-His-

104      His, at the C-terminal, and Dfer_5652 also had 16 residues, Met-Ala-Ser-Met-Thr-Gly-Gly-Gln-Gln-Met-

105      Gly-Arg-Gly-Ser-Glu-Phe at the N-terminal. The DNA sequences of the insert and its flanking regions

106      were verified by sequence analysis using an Applied Biosystems 3130 Genetic Analyzer (Life

107      Technologies, Carlsbad, CA, USA).

108

109      *Preparation of recombinant enzymes*

110        Recombinant Runsl_4512 and Dfer_5652 were produced in transformant of *Escherichia coli* BL21

111      (DE3) carrying their expression plasmids. The transformants were grown in LB medium containing 100

112      μg/mL ampicillin, at 37 °C (1 L for Runsl_4512 and 6 L for Dfer_5652). Recombinant proteins were

113      produced by adding 0.1 M isopropyl β-D-thiogalactopyranoside to a final concentration of 0.1 mM for

114      Runsl_4512 and 0.05 mM for Dfer_5652, when absorbance at 600 nm reached 0.5. The induction was

115      carried out at 18 °C for 20 h for Runsl_4512, and at 37 °C for 4 h for Dfer_5652. Bacterial cells,

116      harvested via centrifugation at $6000 \times g$ at 4 °C for 10 min, were suspended in 40 mL of 30 mM

117      imidazole-HCl buffer containing 0.5 M NaCl (pH 7.0; buffer A) for Runsl_4512 and 30 mM imidazole-

118      HCl buffer containing 0.3 M NaCl (pH 8.0; buffer B) for Dfer_5652. The cells were disrupted by

119      sonication, and cell debris was removed via centrifugation at $18,000 \times g$ at 4 °C for 10 min. The cell-free

120      extract obtained was applied onto a $Ni^{2+}$-immobilized Chelating Sepharose Fast Flow column (2.8 cm i.d.

121 × 3.0 cm, GE Healthcare, Uppsala, Sweden) equilibrated with buffer A and B for Runsl_4512 and

122 Dfer_5652, respectively. The column was washed with the starting buffer, and the adsorbed protein was

123 eluted in a 30 to 500 mM linear gradient of imidazole (total elution volume, 200 mL). The fractions

124 containing highly purified protein, as demonstrated by SDS-PAGE, were pooled and dialyzed against a 10

125 mM Tris-HCl buffer (pH 7.0). The sample was concentrated to 4–10 mg/mL via ultrafiltration using

126 Vivaspin 20 centrifugal concentrators (nominal molecular weight limit 30,000 Da; Sartorius, Göttingen,

127 Germany). Runsl_4512 was stored at −20 °C in the presence of 50% (v/v) glycerol. Dfer_5652 was stored

128 at 4 °C without glycerol because this enzyme was fully stable under these conditions. Molar

129 concentrations of the purified enzymes were determined to be the average of the protein concentrations,

130 calculated, using Eq. 1, from the number of respective amino acids in one protein molecule and the

131 concentrations of respective amino acids after acid hydrolysis of the purified enzyme in 6 M HCl at

132 110 °C for 24 h.

133 Eq. 1: Protein concentration (μM) = [amino acid concentration, μM]/number of amino acid

134 Amino acid concentrations were measured using a JLC-500/V amino acid analyzer (JEOL, Tokyo,

135 Japan).

136 D187N mutation in Runsl_4512 was introduced with a Primestar Mutagenesis Basal Kit (Takara

137 Bio). The expression plasmid of Runsl_4512 as template and primers, as listed in Table 1, were used. The

138 mutant enzyme was prepared in a similar manner as the wild type.

139

140 *Blue native PAGE*

141        The purified Runsl_4512 and Dfer_5652 were evaluated by using blue native PAGE (BN-PAGE)

142    (Schägger et al. 1994). The analytical sample was prepared using a Native PAGE Sample Prep Kit (Life

143    Technologies). Native PAGE Novex 4– 16% Bio-Tris Gels (Life Technologies) were used and

144    electrophoresis was performed at a constant 150 V for 115 min on ice. Native Mark Unstained Standard

145    (Life Technologies) was used as protein molecular size standards.

146

147    *Screening of substrates*

148        Activity of various substrates was examined via TLC and high-performance anion exchange

149    chromatography with pulsed amperometric detection (HPAEC-PAD). For TLC analysis, a reaction

150    mixture (5 μL), containing 0.68–0.83 μM enzyme, 50 mM substrate [D-lyxose, D-mannose, D-glucose, D-

151    tagatose, D-xylose (Wako Pure Chemical Industries, Osaka, Japan); D-talose, D-xylulose (Sigma, St.

152    Louis, MO, USA); D-fructose, D-galactose (Nacalai Tesque, Kyoto, Japan); β-(1→4)-mannobiose,

153    prepared as described previously (Kawahara et al. 2012)], and 5 mM Tris-HCl buffer (pH 8.0), was

154    incubated at 37 °C for 4 h. About 1 μL of the sample was spotted on a silica gel plate (TLC Silica gel 60

155    $F_{254}$ Aluminium sheet, Merck, Darmstadt, Germany) and developed by 2-propanose/1-butanol/water

156    (2/2/1, v/v/v). Sugars were detected by spraying a detection reagent [acetic acid/sulfuric

157    acid/anisaldehyde (100/2/1, v/v/v)] onto the plate, followed by heating of the plate. For HPAEC-PAD

158    analysis, a reaction mixture (50 μL), containing 0.87–1.37 μM enzyme, 50 mM substrate [*N*-acetyl-D-

159    glucosamine (Nacalai Tesque); *N*-acetyl-D-mannosamine, D-glucosamine (Tokyo Chemical Industry,

160    Tokyo, Japan); and D-mannosamine (Wako Pure Chemical Industries)], and 40 mM HEPES-NaOH buffer

8

161 (pH 8.0), was incubated at 37 °C for 12 h. The reaction mixture was analyzed using HPAEC-PAD under

162 following conditions: injection volume, 10 μL (10-fold diluted sample with water); column, Carbopac

163 PA1 (4 mm i.d. × 250 mm; Thermo Fischer Scientific, Waltham, MA, USA); eluent, 18 mM NaOH; flow

164 rate, 1 mL/min.

165

166 *ME activity assay*

167 The activity of epimerization to D-mannose was measured. A reaction mixture (100 μL) containing

168 enzyme, 10 mM D-mannose, and 40 mM HEPES-NaOH (pH 8.0) was incubated at 37 °C for 20 min. The

169 enzyme reaction was stopped by heating at 80 °C for 3 min, and 50 μL of the supernatant, obtained by

170 centrifuging the reaction mixture at 13,000 × $g$ at 4 °C for 5 min, was mixed with 50 μL of a mixture

171 comprising 1 mM thio-NAD$^+$ (Wako Pure Chemical Industries), 2 U/mL hexokinase (Nacalai Tesque), 2

172 U/mL glucose 6-phosphate dehydrogenase (Nacalai Tesque), 14 mM ATP (Sigma), 0.2 M Tris-HCl buffer

173 (pH 7.5), and 20 mM MgCl$_2$. This solution was incubated at 37 °C for 20 min, and its absorbance at 405

174 nm was measured. As a standard, 0–100 μM D-glucose containing 10 mM D-mannose was used. One unit

175 (U) of enzyme activity was defined as an enzyme amount producing 1 μmol of D-mannose in 1 min under

176 these conditions.

177 Kinetic parameters for the epimerization of D-mannose were determined from the reaction rates as

178 4–100 mM D-mannose. The Michaelis–Menten equation was fitted to the reaction rates by nonlinear

179 regression using the Grafit ver. 7.0.2 software (Erithacus Software, East Grinstead, UK).

180

181    *Assaying the epimerization activity of D-mannose 6-phosphate*

182        A reaction mixture (200 μL), containing enzyme, 10 mM D-mannose 6-phosphate disodium salt

183    (Sigma), and 40 mM HEPES-NaOH buffer (pH 8.0), was incubated at 37 °C for 30 min. Fifty μL of the

184    reaction mixture was collected every 10 min and heated at 100 °C for 3 min to stop the reaction. D-

185    Glucose 6-phosphate was quantified as follows: 50 μL of the sample was mixed with 20 μL of mixture

186    containing 2.5 mM thio-NAD$^+$ and 5 U/mL D-glucose 6-phosphate dehydrogenase, and was then

187    incubated at 37 °C for 30 min. Absorbance at 405 nm was measured, and D-glucose 6-phosphate

188    concentration was calculated from a standard curve of D-glucose 6-phosphate disodium salt (0–250 μM;

189    Oriental Yeast, Tokyo, Japan).

190

191    *Effects of pH and temperature on activity and stability*

192        Optimum pH was determined from the activities at various pH values. The pH of the reaction was

193    varied using 100 mM Britton–Robinson buffer (pH 4.0–11.0) as reaction buffer. Optimum temperature

194    was evaluated based on the activity at 20–70 °C. Residual activities after the pH and heat treatments were

195    measured to evaluate the enzyme stability. During the pH treatment, the enzyme solution was incubated at

196    pH 2.3–12.1 using 50 mM Britton–Robinson buffer at 4 °C for 24 h; whereas, during the heat treatment,

197    the enzyme solution was incubated at 20–100 °C for 20 min. The pH and temperature ranges, in which

198    the enzyme retained more than 90% of its original activity, were regarded as stable ranges.

199

200    *Production of D-mannose from D-glucose*

201    A reaction mixture (1 mL) containing 500 g/L D-glucose, 0.25 U/mL Runsl_4512 or Dfer_5652, and

202    50 mM HEPES-NaOH (pH 8.0) was incubated at 50 °C for 48 h. One hundred μL of the reaction mixture

203    was collected at a stipulated time, diluted with water 10 times, and heated at 100 °C for 5 min to stop the

204    reaction. The sugar content of the reaction mixture was analyzed via HPLC under the following

205    conditions: sample injection volume, 10 μL; column, Hilic Pac VG50 4E (4.6 mm i.d. × 250 mm;

206    Shodex, Tokyo, Japan); column temperature, 40 °C; eluent, 80% (v/v) acetonitrile; flow rate, 0.6 mL/min;

207    and detection, refractive index. Authentic D-glucose, D-mannose, and D-fructose were used as standards.

208

209    *NMR analysis of the reaction products of Runsl_4512*

210    The epimerization of D-mannose and D-glucose by Runsl_4512 was monitored by $^1$H-NMR. $H_2O$ in

211    the enzyme solution was replaced with $^2H_2O$: the enzyme solution was diluted with 10 mM HEPES-

212    NaO$^2$H buffer in $^2H_2O$ (p$^2$H 8.0) by 3-fold and was further concentrated to the original volume via

213    ultrafiltration as aforementioned. These steps were repeated four times in total. $^1$H-NMR of a reaction

214    mixture (0.5 mL), containing Runsl_4512 (23 and 73 μM for the reactions with D-mannose and D-

215    glucose, respectively), 250 mM substrate, and 10 mM HEPES-Na buffer (p$^2$H 8.0), was recorded at 27 °C

216    using Bruker AMX500 (Billerica, MA, USA). In the reactions with D-glucose and D-mannose, 22.5 mg of

217    substrate powder was dissolved in 50 μL of $^2H_2O$ and incubated at 25 °C for 24 h to obtain the

218    equilibrium mixture of α- and β-anomers. This substrate solution was mixed with 450 μL of the enzyme

219    solution in 10 mM HEPES-NaO$^2$H buffer (p$^2$H 8.0), and this mixture was immediately subjected to the

220    $^1$H-NMR analysis. In the reactions with α-D-glucose (Sigma) and β-D-glucose (Sigma), 22.5 mg of sugar

221 was dissolved with 0.5 mL of the enzyme solution in 10 mM HEPES-NaO$^2$H buffer (p$^2$H 8.0) just before

222 the reactions.

223    The reaction mixture with D-mannose was incubated at 25 °C for 24 h to prepare an equilibrium

224 reaction mixture. $^1$H-NMR of this mixture was recorded, and the spectrum was compared with the

225 equimolar mixture (250 mM) of D-glucose and D-mannose. This reaction mixture was dried up under

226 reduced pressure, and the residue was dissolved in H$_2$O. $^2$H-NMR was recorded to detect $^2$H in the

227 reaction products.

228

229 **Results**

230 *Determination of catalytic activity of Runsl_4512 and Dfer_5652*

231    Runsl_4512 and Dfer_5652, belonging to a cluster of uncharacterized proteins in a phylogenetic

232 analysis of AGE superfamily enzymes (Fig. 1), were emphasized in this study. The amino acid sequence

233 of Runsl_4512 is 74% identical with that of Dfer_5652, and sequence identities of Runsl_4512 and

234 Dfer_5652 with characterized AGE superfamily members are as follows: *Ruminococcus albus* CE, 24%

235 and 24%; *Rhodothermus marinus* CE, 25% and 25%; *Anabaena* sp. AGE, 16% and 17%; *E. coli* SQI,

236 14% and 13%; *Marinomonas mediterranea* MI, 18% and 19%; and *Thermobifida fusca* MI, 12% and

237 17%, respectively.

238    To investigate the enzymatic functions of Runsl_4512 and Dfer_5652, recombinant enzymes were

239 produced in *E. coli* transformant, and purified. These proteins were displayed as single bands on SDS-

240 PAGE and BN-PAGE (Fig. 2). The molecular masses of Runsl_4512 and Dfer_5652 were estimated to be

241   45 kDa (theoretical molecular mass, 50 kDa) and 47 kDa (theoretical molecular mass, 52 kDa) on SDS-

242   PAGE, and 81 kDa and 101 kDa on BN-PAGE, respectively. These results suggested that Runsl_4512 and

243   Dfer_5652 exist as homodimers under nondenaturing conditions. The purified samples were then

244   incubated with various carbohydrates to find their substrates, and D-mannose and D-glucose were detected

245   as the reaction products from D-glucose and D-mannose, respectively (Fig. 3). This result indicates that

246   these proteins catalyzed the epimerization of D-mannose (ME reaction). No reaction products were

247   detected in the reactions with D-galactose, D-talose, D-xylose, D-lyxose, D-glucosamine, D-mannosamine,

248   $N$-acetyl-D-glucosamine, $N$-acetyl-D-mannosamine, β-(1→4)-mannobiose, D-mannose 6-phosphate, D-

249   fructose, D-tagatose, and D-xylulose.

250   Enzymatic properties of Runsl_4512 and Dfer_5652 were investigated based on the ME activity. The

251   ME activity at pH 4.0–11.0 was measured to evaluate the optimum pH. Runsl_4512 and Dfer_5652 were

252   most active at pH 7.8 and 8.1, respectively. Optimum temperature was evaluated based on the activity at

253   20–70 °C. Both enzymes exhibited highest activity at 37 °C. Stable pH and temperature ranges of these

254   enzymes were pH 6.3–10 (4 °C for 24 h) and at ≤40 °C (pH 8.0 for 20 min), respectively. The Michaelis–

255   Menten equation fitted well with the reaction rates of Runsl_4512 and Dfer_5652 at various D-mannose

256   concentrations (Fig. 4). The $K_m$ values were determined from the concentration of D-mannose, including

257   both α- and β-anomers. The $k_{cat}$ and $K_m$ of Runsl_4512 were 286 min$^{-1}$ and 73.5 mM, and those of

258   Dfer_5652 were 233 min$^{-1}$ and 66.4 mM, respectively (Table 2).

259

260   *Production of D-mannose from D-glucose*

261        D-Mannose was enzymatically synthesized from 500 g/L D-glucose (Fig. 5). The concentrations of D-

262        mannose reached 122 g/L and 114 g/L, 48-h after reaction with Runsl_4512 and Dfer_5652, respectively.

263        Molar rates of conversion to D-mannose using Runsl_4512 and Dfer_5652 were 24.4% and 22.8%,

264        respectively. Faint D-fructose production was observed: D-fructose concentrations after 48-h reactions

265        with Runsl_4512 and Dfer_5652 were 8.5 and 7.9 g/L, respectively. These D-fructose concentrations were

266        consistent with those observed after a 48-h reaction without enzyme 8.3 g/L. Thus, the D-fructose

267        generated in ME reaction mixtures was regarded as a nonenzymatic reaction product. Nonenzymatic

268        epimerization was not observed under the reaction conditions.

269

270        *NMR analysis of the reaction products by Runsl_4512*

271        The anomeric configuration of the products of reactions carried out using Runsl_4512 was analyzed

272        through ^{1}H-NMR. In the reactions with D-mannose and D-glucose (equilibrium mixture of α- and β-

273        forms), the 1-H signals of β-D-glucose (4.63 ppm) and β-D-mannose (4.88 ppm) were detected from the

274        initial stage of the reactions whereas the 1-H signals of α-D-glucose (5.22 ppm) and α-D-mannose (5.18

275        ppm) were not (Fig. 6A and B). This result indicates that β-D-glucose and β-D-mannose were produced

276        from D-mannose and D-glucose, respectively. Production of the epimerized product from α- and β-D-

277        glucose was monitored (Fig. 6C and D). The 1-H signal of β-D-mannose was detected at the initial stage

278        of the reaction with β-D-glucose, but in the reaction with α-D-glucose, this signal was scarce and was only

279        observed in the later stages, along with the production of β-D-glucose. Thus, Runsl_4512 used β-D-

280        glucose as the substrate.

281    The equilibrium reaction mixture, produced from D-mannose in $^2H_2O$, was analyzed by $^1H$- and $^2H$-

282    NMR analyses (Fig. 6E). In the $^1H$-NMR spectrum of the equilibrium reaction mixture, 2-H signals of D-

283    mannose (3.9 ppm) and D-glucose (3.2 ppm and 3.5 ppm for β- and α-D-glucose, respectively) were not

284    detected, whereas $^2H$ signals were clearly detected at the corresponding chemical shifts of the 2-H of D-

285    mannose and D-glucose by $^2H$-NMR. This result indicates that Runsl_4512 abstracts 2-H from the

286    substrates and adds $^2H$ from the reaction solvent.

287

288    *Site-directed mutagenesis at Asp187 of Runsl_4512*

289    Multiple sequence alignment of AGE superfamily enzymes was carried out to compare the amino

290    acid sequences of MEs with those of the other members (Fig. 7). His273 and His404 of Runsl_4512 and

291    Dfer_5652 correspond to the catalytic His residues of known enzymes, which are situated on the 8th and

292    12th α-helices of the catalytic $(\alpha/\alpha)_6$-barrel domain. Arg60, Tyr119, His191, Glu276, and Trp336 of

293    Runsl_4512 and Dfer_5652 also correspond to the substrate-binding residues of CE, MI, and SQI, which

294    act on the substrates harboring 2-OH group. Nevertheless, in the ME sequences, Asp187 was observed as

295    the equivalent residue of Asn on α-helix 6 of CE, MI, and SQI, which has a hydrogen bonding interaction

296    with 2-OH of substrates (Fujiwara et al. 2014, Itoh et al. 2008). D187N mutant of Runsl_4512 was

297    prepared to evaluate the importance of Asp187. The activity of this mutant enzyme to 10 mM D-mannose

298    was not detectable (<0.002 U/mg), while that of wild type was 0.61 U/mg. Thus, Asp187 is essential for

299    the catalytic activity of Runsl_4512.

300

**Discussion**

301

302        Carbohydrate epimerization and isomerization are essential reactions to convert abundant

303    sugars into rare sugars. In this study, reversible 2-epimerization activity between D-mannose and D-

304    glucose was observed in Runsl_4512 and Dfer_5652 proteins belonging to a yet uncharacterized protein

305    cluster of AGE superfamily (Fig. 1). This activity was also detected in several CEs (Park et al. 2011;

306    Saburi et al. 2015); however, the $k_{cat}/K_m$ values of Runsl_4512 and Dfer_5652 were 4.1–140-fold higher

307    than CEs from *Caldicellulosiruptor saccharolyticus* and *Cellvibrio vulgaris* (Table 2). In contrast to CEs,

308    Runsl_4512 and Dfer_5652 did not present any detectable epimerization activity to β-(1→4)-linked

309    disaccharides.

310        Sequence comparison between MEs and function-known AGE superfamily enzymes revealed that

311    the MEs have residues corresponding to two catalytic His residues and a majority of residues important

312    for substrate-binding in MI, SQI, and CE (Fig. 7); ME presumably shares the mechanisms of substrate

313    binding and catalysis with these enzymes. Among the possible residues involved in the substrate binding,

314    only Asp187 of Runsl_4512 and Dfer_5652 differs from the corresponding residue of CE and MI as

315    aforementioned. As Asp187 was confirmed to be essential for the catalytic activity through D187N

316    mutation in Runsl_4512, it might have specific function for ME activity. Multiple-sequence alignment

317    suggests that ME has a longer loop connecting the 7th and 8th α-helices (α7→α8 loop) than any

318    characterized AGE superfamily member (Fig. 7). In MI, the corresponding loop is predicted to cause

319    steric hindrance upon binding to the disaccharide substrate (Saburi et al. 2018). Therefore, long α7→α8

320    loop of ME might be important for the monosaccharide specificity. Three-dimensional structure analysis

16

321    of MEs would provide essential information to understand the structure–function relationship of this

322    enzyme.

323        Analysis of anomeric configuration of the reaction product by ${}^1$H-NMR revealed that ME forms the

324    product of β-anomer. This anomeric configuration of the reaction product is in accordance with that of β-

325    (1→4)-disaccharides bound to CE (Fujiwara et al. 2014), and the isomerized product, D-mannose, from

326    D-fructose by MI (Saburi et al. 2018). In the reaction with β-D-glucose, β-D-mannose was formed from

327    the initial stage of the reaction; however, this was not observed in the reaction with α-D-glucose. Thus,

328    ME utilizes β-glucose as a substrate, that is, the anomeric configuration of the substrate is retained in the

329    product. Slight production of β-D-mannose in the later stage of the reaction with α-D-glucose is

330    presumably attributable to the reaction with β-D-glucose, generated from α-D-glucose via mutarotation.

331    Retention of β-anomer in the substrate and product is presumably suitable for the ring opening and

332    closure mechanism catalyzed by His on the 12th α-helix as general acid/base catalyst, which forms

333    hydrogen bonds with 1-O and 5-O of the substrate of β-anomer (Fujiwara et al. 2014).

334        The NMR analysis of the equilibrated reaction product indicated that 2-H of the substrate was

335    substituted with ${}^2$H from solvent ${}^2$H$_2$O, indicating that ME epimerizes the substrate via proton abstraction

336    and addition mechanisms as postulated in CE and AGE (Lee et al. 2007; Fujiwara et al. 2014). Based on

337    the sequence comparison between ME and CE, it is predicted that His273 of Runsl_4512 and Dfer_5652

338    serves as general base catalyst to abstract 2-H from D-mannose and produce *cis*-endiolate intermediate,

339    and His404 serves as general acid catalyst to donate proton to the intermediate and produce D-glucose

340    (Fig. 8).

341    D-Mannose has several beneficial physiological properties, such as preventing urinary tract

342    infections (Kranjčec et al. 2014) and treating phosphomannose isomerase deficient induced congenital

343    disorders of glycosylation (de Lonlay and Seta 2009), and it could be widely applied as an important

344    intermediate for synthesizing immunostimulatory agents (Ranta et al. 2012), vitamin (Chen et al. 2007),

345    and D-mannitol (Ghoreishi and Shahrestani 2009). Furthermore, D-mannose is useful as an animal feed

346    for suppressing *Salmonella* contamination (Oyofo et al. 1989). Since the decomposition of an abundant

347    naturally occurring D-mannose polymer, β-mannan, requires rigorous conditions, the enzymatic

348    production of D-mannose from other monosaccharides, especially D-glucose, is useful. Isomerization of

349    D-fructose by MI (Hirose et al. 2003; Hu et al. 2016), D-lyxose isomerase (Park et al. 2010a), and L-

350    rhamnose isomerase (Park et al. 2010b) and the epimerization of D-glucose to D-mannose by CE (Park et

351    al. 2011) have been reported to date. The production yield of D-mannose from 200–500 g/L D-fructose

352    through isomerization by the abovementioned isomerases at 45–85°C and pH 7.0–8.0 was 20–35%

353    (molar ratio). As D-fructose is produced from D-glucose by enzymatic isomerization at 60°C and pH 6.0–

354    8.0 using D-xylose isomerase, at approximately 40% yield (molar ratio; Bhosale et al. 1996), the

355    production yield of D-mannose from D-glucose through two-step isomerization, is estimated to be 8–14%

356    (molar ratio). In fact, that of D-mannose by the coupling reaction of D-xylose isomerase and D-lyxose

357    isomerase with 400 g/L D-glucose at 55°C and pH 6.5 was reported to be 16% (Huang et al. 2018). In D-

358    mannose production from 500 g/L D-glucose at 75°C and pH 7.5 by *C. saccharolyticus* CE, the yield of

359    D-mannose from D-glucose was only 15% (molar ratio) due to its isomerization activity (yield of D-

360    fructose was 9.5%) (Park et al. 2011). Isomerization activity was not detected in MEs under the analytical

361 conditions, and the production yield of D-mannose from 500 g/L D-glucose at 50°C and pH 8.0 by ME

362 (23–24%, molar ratio) was higher than that observed for the reactions previously reported. Thus, ME is a

363 useful biocatalyst for enzymatic D-mannose production, and further study of ME for application in D-

364 mannose production could provide a new and efficient synthetic pathway for D-mannose.

365

379

380 **References**

381  Bhosale SH, Rao MB, Deshpande VV (1996) Molecular and industrial aspects of glucose isomerase.

382  Microbiol Rev 60:280-300.

383  Chen FE, Zhao JF, Xiong FJ, Xie B, Zhang P (2007) An improved synthesis of a key intermediate for (+)-

384  biotin from D-mannose. Carbohydr Res 342:2461-2464. doi: 10.1016/j.carres.2007.06.029

385  de Lonlay P, Seta N (2009) The clinical spectrum of phosphomannose isomerase deficiency, with an

386  evaluation of mannose treatment for CDG-Ib. Biochim Biophys Acta 1792:841-843. doi:

387  10.1016/j.bbadis.2008.11.012

388  Denger K, Weiss M, Felux AK, Schneider A, Mayer C, Spiteller D, Huhn T, Cook AM, Schleheck D (2014)

389  Sulphoglycolysis in *Escherichia coli* K-12 closes a gap in the biogeochemical sulphur cycle. Nature

390  507:114-117. doi: 10.1038/nature12947

391  Fujiwara T, Saburi W, Inoue S, Mori H, Matsui H, Tanaka I, Yao M (2013) Crystal structure of

392  *Ruminococcus albus* cellobiose 2-epimerase: structural insights into epimerization of unmodified sugar.

393  FEBS Lett 587:840-846. doi: 10.1016/j.febslet.2013.02.007

394  Fujiwara T, Saburi W, Matsui H, Mori H, Yao M (2014) Structural insights into the epimerization of β-1,4-

395  linked oligosaccharides catalyzed by cellobiose 2-epimerase, the sole enzyme epimerizing non-anomeric

396  hydroxyl groups of unmodified sugars. J Biol Chem 289:3405-3415. doi: 10.1074/jbc.M113.531251

397  Ghoreishi SM, Shahrestani RG (2009) Innovative strategies for engineering mannitol production. Trends

398  Food Sci Tech 20:263-270. doi: 10.1016/j.tifs.2009.03.006

399  Hirose J, Kinoshita Y, Fukuyama S, Hayashi S, Yokoi H, Takasaki Y (2003) Continuous isomerization of

400  D-fructose to D-mannose by immobilized *Agrobacterium radiobacter* cells. Biotechnol Lett 25:349-352.

401 doi: 10.1023/A:1022301725817

402 Hu X, Zhang P, Miao M, Zhang T, Jiang B (2016) Development of a recombinant D-mannose isomerase

403 and its characterizations for D-mannose synthesis. Int J Biol Macromol 89:328-335. doi:

404 10.1016/j.ijbiomac.2016.04.083

405 Huang J, Yu L, Zhang W, Zhang T, Guang C, Mu W (2018) Production of D-mannose from D-glucose by

406 co-expression of D-glucose isomerase and D-lyxose isomerase in *Escherichia coli*. J Sci Food Agric

407 98:4895-4902. doi: 10.1002/jsfa.9021

408 Iida T, Hayashi N, Yamada T, Yoshikawa Y, Miyazato S, Kishimoto Y, Okuma K, Tokuda M, Izumori K

409 (2010) Failure of D-psicose absorbed in the small intestine to metabolize into energy and its low large

410 intestinal fermentability in humans. Metabolism 59:206-214. doi: 10.1016/j.metabol.2009.07.018

411 Ito S, Taguchi H, Hamada S, Kawauchi S, Ito H, Senoura T, Watanabe J, Nishimukai M, Ito S, Matsui H

412 (2008) Enzymatic properties of cellobiose 2-epimerase from *Ruminococcus albus* and the synthesis of rare

413 oligosaccharides by the enzyme. Appl Microbiol Biotechnol 79:433-441. doi: 10.1007/s00253-008-1449-

414 7

415 Itoh T, Mikami B, Hashimoto W, Murata K (2008) Crystal structure of YihS in complex with D-mannose:

416 structural annotation of *Escherichia coli* and *Salmonella enterica yihS*-encoded proteins to an aldose-ketose

417 isomerase. J Mol Biol 377:1443-1459. doi: 10.1016/j.jmb.2008.01.090

418 Itoh T, Mikami B, Maru I, Ohta Y, Hashimoto W, Murata K (2000) Crystal structure of *N*-acyl-D-

419 glucosamine 2-epimerase from porcine kidney at 2.0 Å resolution. J Mol Biol 303:733-744. doi:

420 10.1006/jmbi.2000.4188

21

421  Kasumi T, Mori S, Kaneko S, Matsumoto H, Kobayashi Y, Koyama Y (2014) Characterization of mannose

422  isomerase from a cellulolytic actinobacteria *Thermobifida fusca* MBL10003. J Appl Glycosci 61:21-25.

423  doi: 10.5458/jag.jag.JAG-2013_008

424  Katoh K, Rozewicki J, Yamada KD (2017) MAFFT online service: multiple sequence alignment, interactive

425  sequence choice and visualization. Brief Bioinform. doi: 10.1093/bib/bbx108

426  Kawahara R, Saburi W, Odaka R, Taguchi H, Ito S, Mori H, Matsui H (2012) Metabolic mechanism of

427  mannan in a ruminal bacterium, *Ruminococcus albus*, involving two mannoside phosphorylases and

428  cellobiose 2-epimerase. Discovery of a new carbohydrate phosphorylase, β-1,4-mannooligosaccharide

429  phosphorylase. J Biol Chem 287:42389-42399. doi: 10.1074/jbc.M112.390336

430  Kiyohara M, Tachizawa A, Nishimoto M, Kitaoka M, Ashida H, Yamamoto K. (2009) Prebiotic effect of

431  lacto-*N*-biose I on bifidobacterial growth. Biosci Biotechnol Biochem 73:1175-1179. doi:

432  10.1271/bbb.80697

433  Kranjčec B, Papeš D, Altarac S (2014) D-mannose powder for prophylaxis of recurrent urinary tract

434  infections in women: a randomized clinical trial. World J Urol 32:79-84. doi: 10.1007/s00345-013-1091-6

435  Kuyper M, Winkler AA, van Dijken JP, Pronk JT (2004) Minimal metabolic engineering of *Saccharomyces*

436  *cerevisiae* for efficient anaerobic xylose fermentation: a proof of principle. FEMS Yeast Res 4:655-664.

437  doi: 10.1016/j.femsyr.2004.01.003

438  Lee YC, Wu HM, Chang YN, Wang WC, Hsu WH (2007) The central cavity from the (alpha/alpha)$_6$ barrel

439  structure of *Anabaena* sp. CH1 *N*-acetyl-D-glucosamine 2-epimerase contains two key histidine residues

440  for reversible conversion. J Mol Biol 367:895-908. doi: 10.1016/j.jmb.2006.11.001

441  Murakami Y, Ojima-Kato T, Saburi W, Mori H, Matsui H, Tanabe S, Suzuki T (2015) Supplemental

442  epilactose prevents metabolic disorders through uncoupling protein-1 induction in the skeletal muscle of

443  mice fed high-fat diets. Br J Nutr 114:1774-1783. doi: 10.1017/S0007114515003505

444  Nishimoto M, Kitaoka M (2007) Practical preparation of lacto-*N*-biose I, a candidate for the bifidus factor

445  in human milk. Biosci Biotechnol Biochem 71:2101-2104. doi: 10.1271/bbb.70320

446  Nishimukai M, Watanabe J, Taguchi H, Senoura T, Hamada S, Matsui H, Yamamoto T, Wasaki J, Hara H,

447  Ito S (2008) Effects of epilactose on calcium absorption and serum lipid metabolism in rats. J Agric Food

448  Chem 56:10340-10345. doi: 10.1021/jf801556m

449  Ochiai M, Nakanishi Y, Yamada T, Iida T, Matsuo T (2013) Inhibition by dietary D-psicose of body fat

450  accumulation in adult rats fed a high-sucrose diet. Biosci Biotechnol Biochem 77:1123-1126. doi:

451  10.1271/bbb.130019

452  Ochiai M, Onishi K, Yamada T, Iida T, Matsuo T (2014) D-Psicose increases energy expenditure and

453  decreases body fat accumulation in rats fed a high-sucrose diet. Int J Food Sci Nutr 65:245-250. doi:

454  10.3109/09637486.2013.845653

455  Oyofo BA, DeLoach JR, Corrier DE, Norman JO, Ziprin RL, Mollenhauer HH (1989) Prevention of

456  *Salmonella typhimurium* colonization of broilers with D-mannose. Poult Sci 68:1357-1360. doi:

457  10.3382/ps.0681357

458  Park CS, Kim JE, Choi JG, Oh DK (2011) Characterization of a recombinant cellobiose 2-epimerase from

459  *Caldicellulosiruptor saccharolyticus* and its application in the production of mannose from glucose. Appl

460  Microbiol Biotechnol 92:1187-1196. doi: 10.1007/s00253-011-3403-3

461     Park CS, Kwon HJ, Yeom SJ, Oh DK (2010a) Mannose production from fructose by free and immobilized

462     D-lyxose isomerases from *Providencia stuartii*. Biotechnol Lett 32:1305-1309. doi: 10.1007/s10529-010-

463     0300-2

464     Park CS, Yeom SJ, Lim YR, Kim YS, Oh DK (2010b) Characterization of a recombinant thermostable L-

465     rhamnose isomerase from *Thermotoga maritima* ATCC 43589 and its application in the production of L-

466     lyxose and L-mannose. Biotechnol Lett 32:1947-1953. doi: 10.1007/s10529-010-0385-7

467     Ranta K, Nieminen K, Ekholm FS, Poláková M, Roslund MU, Saloranta T, Leino R, Savolainen J (2012)

468     Evaluation of immunostimulatory activities of synthetic mannose- containing structures mimicking the β-

469     (1→2)-linked cell wall mannans of *Candida albicans*. Clin Vaccine Immunol 19:1889-1893. doi:

470     10.1128/CVI.00298-12

471     Saburi W (2016) Functions, structures, and applications of cellobiose 2-epimerase and glycoside hydrolase

472     family 130 mannoside phosphorylases. Biosci Biotechnol Biochem 80:1294-1305. doi:

473     10.1080/09168451.2016.1166934

474     Saburi W, Jaito N, Kato K, Tanaka Y, Yao M, Mori H (2018) Biochemical and structural characterization

475     of *Marinomonas mediterranea* D-mannose isomerase Marme_2490 phylogenetically distant from known

476     enzymes. Biochimie 144:63-73. doi: 10.1016/j.biochi.2017.10.016

477     Saburi W, Tanaka Y, Muto H, Inoue S, Odaka R, Nishimoto M, Kitaoka M, Mori H (2015) Functional

478     reassignment of *Cellvibrio vulgaris* EpiA to cellobiose 2-epimerase and an evaluation of the biochemical

479     functions of the 4-*O*-β-D-mannosyl-D-glucose phosphorylase-like protein, UnkA. Biosci Biotechnol

480     Biochem 79:969-977. doi: 10.1080/09168451.2015.1012146

481    Saburi W, Yamamoto T, Taguchi H, Hamada S, Matsui H (2010) Practical preparation of epilactose

482    produced with cellobiose 2-epimerase from *Ruminococcus albus* NE1. Biosci Biotechnol Biochem

483    74:1736-1737. doi: 10.1271/bbb.100353

484    Schägger H, Cramer WA, von Jagow G (1994) Analysis of molecular masses and oligomeric states of

485    protein complexes by blue native electrophoresis and isolation of membrane protein complexes by two-

486    dimensional native electrophoresis. Anal Biochem 217:220–230. doi: 10.1006/abio.1994.1112

487    Standley DM, Toh H, Nakamura H (2007) ASH structure alignment package: Sensitivity and selectivity in

488    domain classification. BMC Bioinformatics 8:116. doi: 10.1186/1471-2105-8-116

489    Suzuki T, Nishimukai M, Shinoki A, Taguchi H, Fukiya S, Yokota A, Saburi W, Yamamoto T, Hara H,

490    Matsui H (2010a) Ingestion of epilactose, a non-digestible disaccharide, improves postgastrectomy

491    osteopenia and anemia in rats through the promotion of intestinal calcium and iron absorption. J Agric Food

492    Chem 58:10787-10792. doi: 10.1021/jf102563y

493    Suzuki T, Nishimukai M, Takechi M, Taguchi H, Hamada S, Yokota A, Ito S, Hara H, Matsui H (2010b)

494    The nondigestible disaccharide epilactose increases paracellular Ca absorption via rho-associated kinase-

495    and myosin light chain kinase-dependent mechanisms in rat small intestines. J Agric Food Chem 58:1927-

496    1932. doi: 10.1021/jf9035063

497    Takeshita K, Suga A, Takada G, Izumori K (2000) Mass production of D-psicose from D-fructose by a

498    continuous bioreactor system using immobilized D-tagatose 3-epimerase. J Biosci Bioeng 90:453-455. doi:

499    10.1016/S1389-1723(01)80018-9

500    Watanabe J, Nishimukai M, Taguchi H, Senoura T, Hamada S, Matsui H, Yamamoto T, Wasaki J, Hara H,

501    Ito S (2008) Prebiotic properties of epilactose. J Dairy Sci 91:4518-4526. doi: 10.3168/jds.2008-1367

502

503    Figure caption

504    **Fig. 1** Phylogenetic analysis of AGE superfamily proteins

505        Proteins of functionally known AGE superfamily enzymes are presented. AGE, acylglucosamine 2-

506    epimerase; CE, cellobiose 2-epimerase; MI, D-mannose isomerase; and SQI, sulfoquinovose isomerase.

507

508    **Fig. 2** SDS-PAGE and BN-PAGE of Runsl_4512 and Dfer_5652

509    Recombinant Runsl_4512 and Dfer_5652, purified from *E. coli* transformant, were analyzed on SDS-

510    PAGE and BN-PAGE. Lane M, R, and D indicate molecular mass standard, Runsl_4512, and

511    Dfer_5652.

512

513    **Fig. 3** TLC analysis of the reaction products by Runsl_4512 and Dfer_5652

514    Plus and minus lanes indicate the reactions with and without the enzyme, respectively. A, Runsl_4512; B,

515    Dfer_5652.

516

517    **Fig. 4** The s-*v* plot for D-mannose epimerization by Runsl_4512 and Dfer_5652

518    Close and open circles indicate Runsl_4512 and Dfer_5652, respectively. Values and error bars are

519    average and standard deviation of three independent experiments.

520

521    **Fig. 5** Time course of production of D-mannose from D-glucose

522    Black circle, D-glucose; white circle, D-mannose; and black triangle, D-fructose. Values indicate mean ±

523    standard deviation for three independent experiments.

524

525    **Fig. 6** NMR analysis of ME reaction products

526    Time course of the ME reaction was monitored using $^1$H-NMR. A, reaction with mixture of α-D-mannose

527    and β-D-mannose; B, reaction with mixture of α-D-glucose and β-D-glucose; C, reaction with α-D-

528    glucose; and D, reaction with β-D-glucose. Reaction time (min) is presented on the left side of the figures.

529    E, $^1$H-NMR and $^2$H-NMR of equilibrated reaction mixture of ME. The spectrum of the equimolar mixture

530    of D-glucose and D-mannose (Man + Glc) is shown as standard.

531

532    **Fig. 7** Multiple sequence alignment of AGE superfamily enzymes

533      Multiple sequence alignment was performed using MAFTFFTash (Standley et al. 2007). The

534    secondary structure is depicted above the sequence. Amino acid residues involved in substrate binding

535    (reducing end part of disaccharides in CE) are presented in bold face. Catalytic His residues are indicated

536    by black circles. Asp187 of Runsl_4512 and Dfer_5652 is indicated by black triangle. RaCE,

537    *Ruminococcus albus* CE; RmCE, *Rhodothermus marinus* CE; MmMI, *Marinomonas mediterranea* MI;

538    TfMI, *Thermobifida fusca* MI; EsSQI, *Escherichia coli* SQI; and AspAGE, *Anabaena* sp. AGE.

539

540    **Fig. 8** Predicted reaction mechanism of ME

541     Arrows indicate electron transfer processes that convert β-D-mannose to β-D-glucose. The bond

542     between 2-C and 3-C would rotate after acceptance of a proton from the general acid catalyst, His404, in

543     the epimerization of D-mannose, according to the reaction mechanism of CE (Fujiwara et al. 2014).
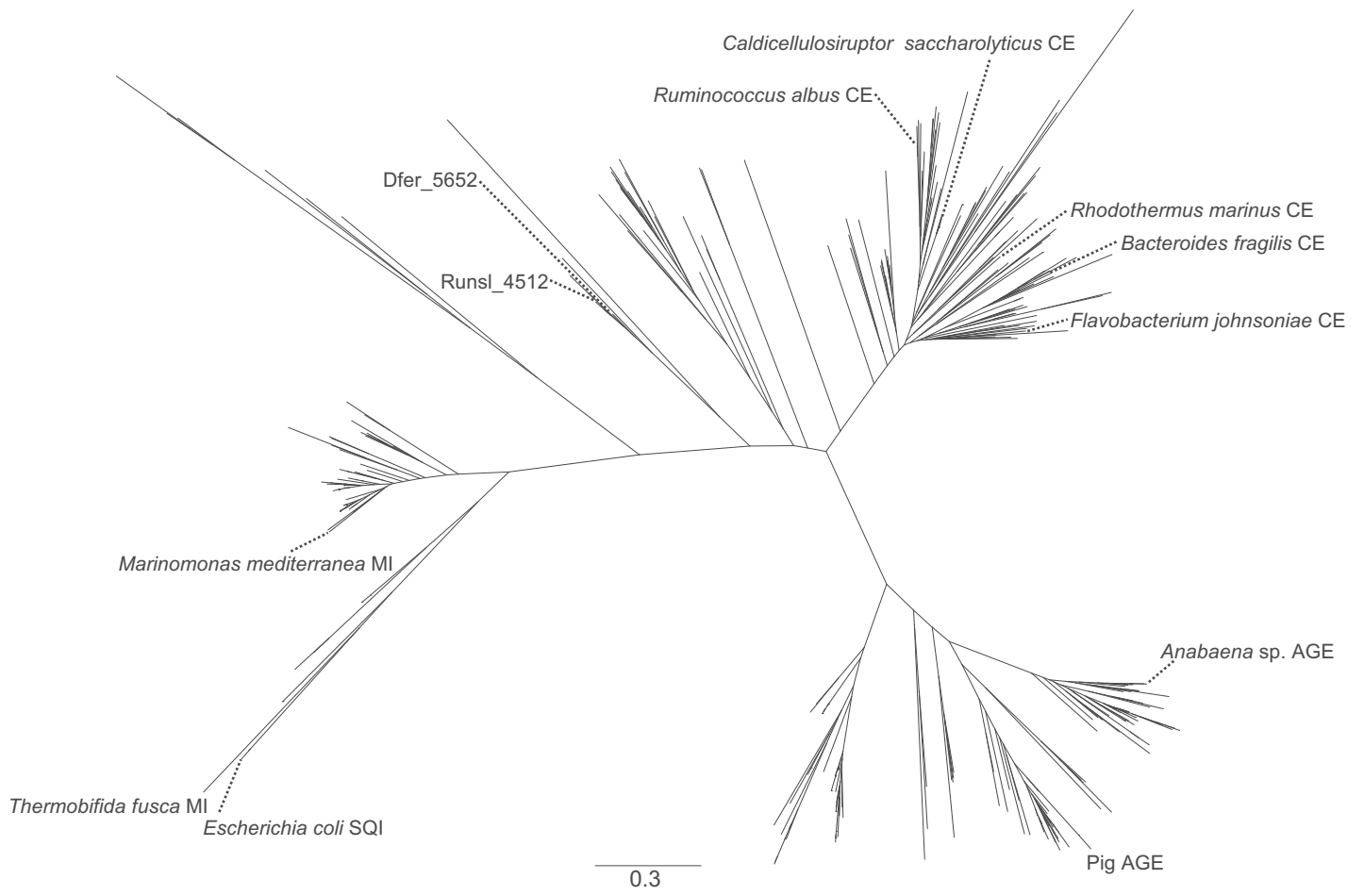
Caldicellulosiruptor  saccharolyticus CE

Ruminococcus albus CE

Dfer_5652

Runsl_4512

Rhodothermus marinus CE

Bacteroides fragilis CE

Flavobacterium johnsoniae CE

Marinomonas mediterranea MI

Anabaena sp. AGE

Thermobifida fusca MI
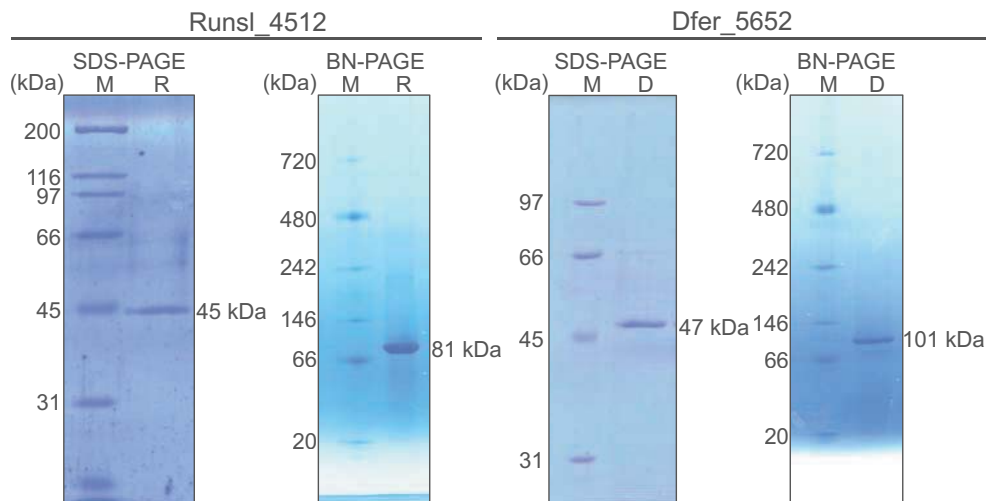
Escherichia coli SQI
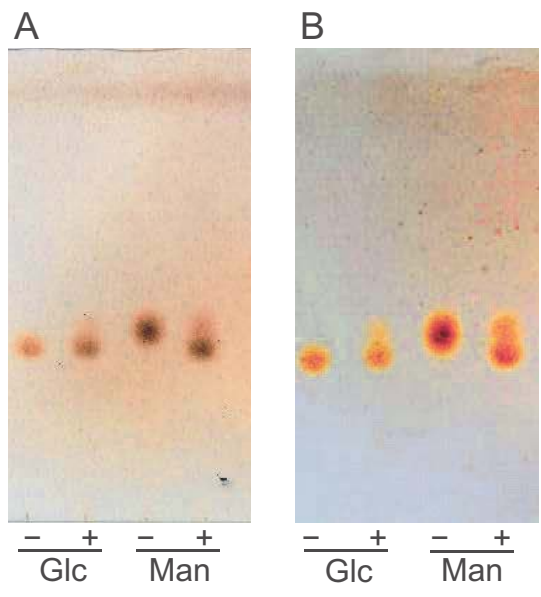
0.3

Pig AGE

Fig. 1, Saburi et al.
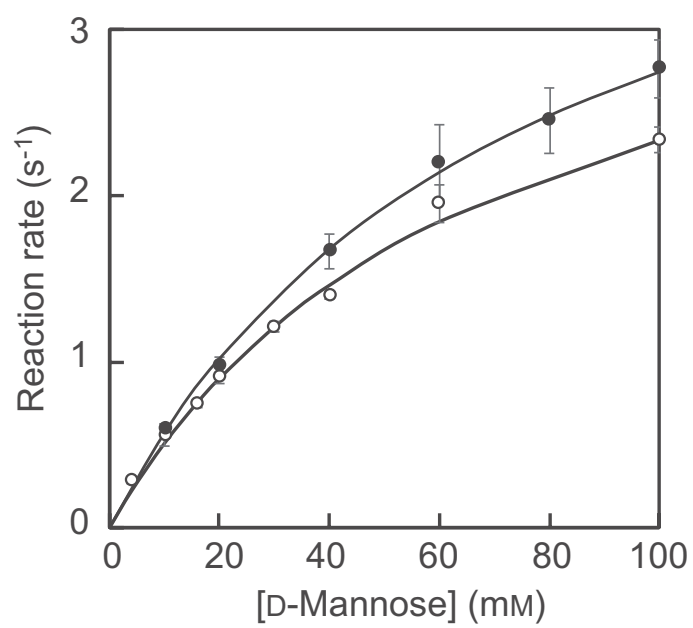
Fig. 2., Saburi et al.

Fig. 3., Saburi et al.

Fig. 4., Saburi et al.

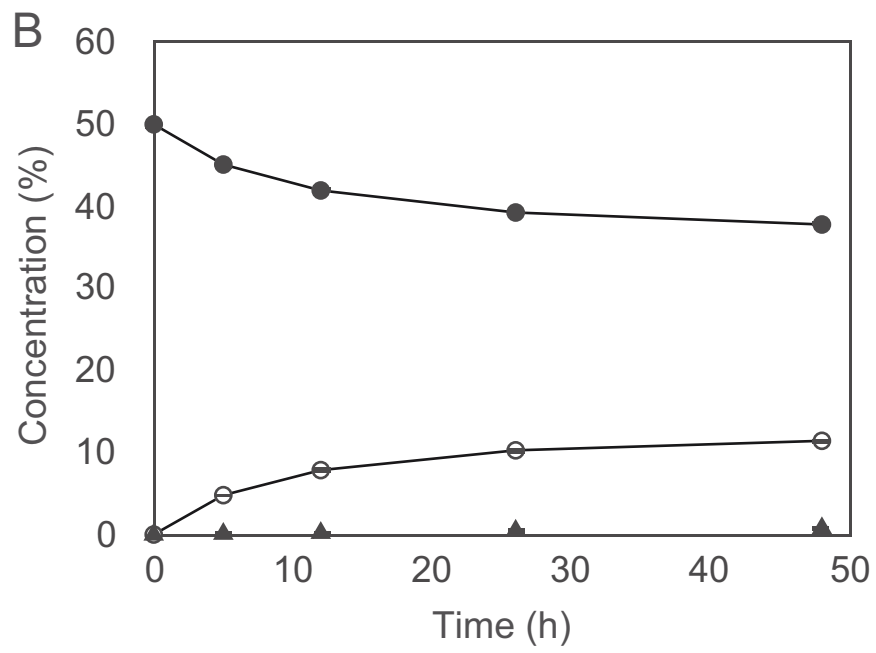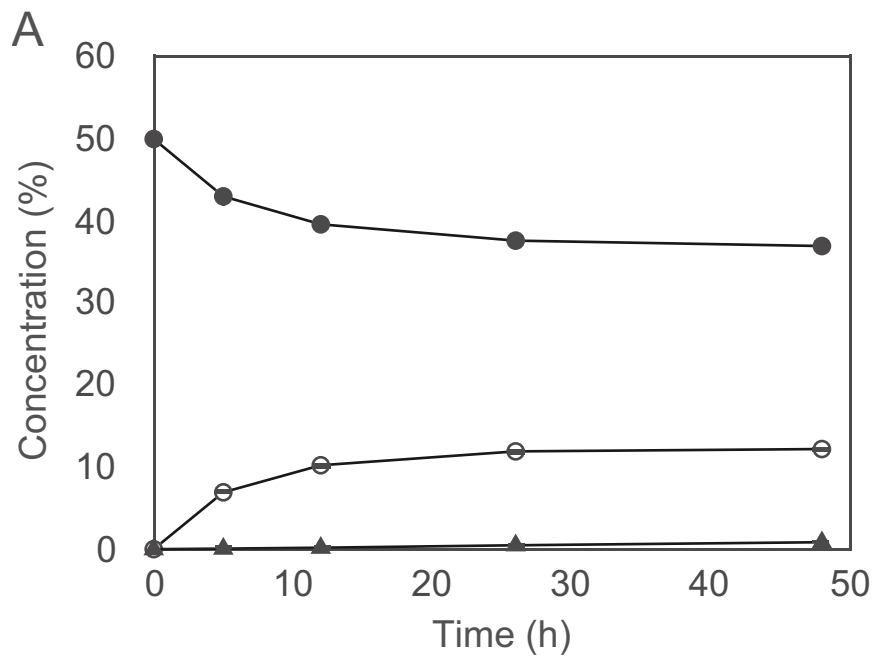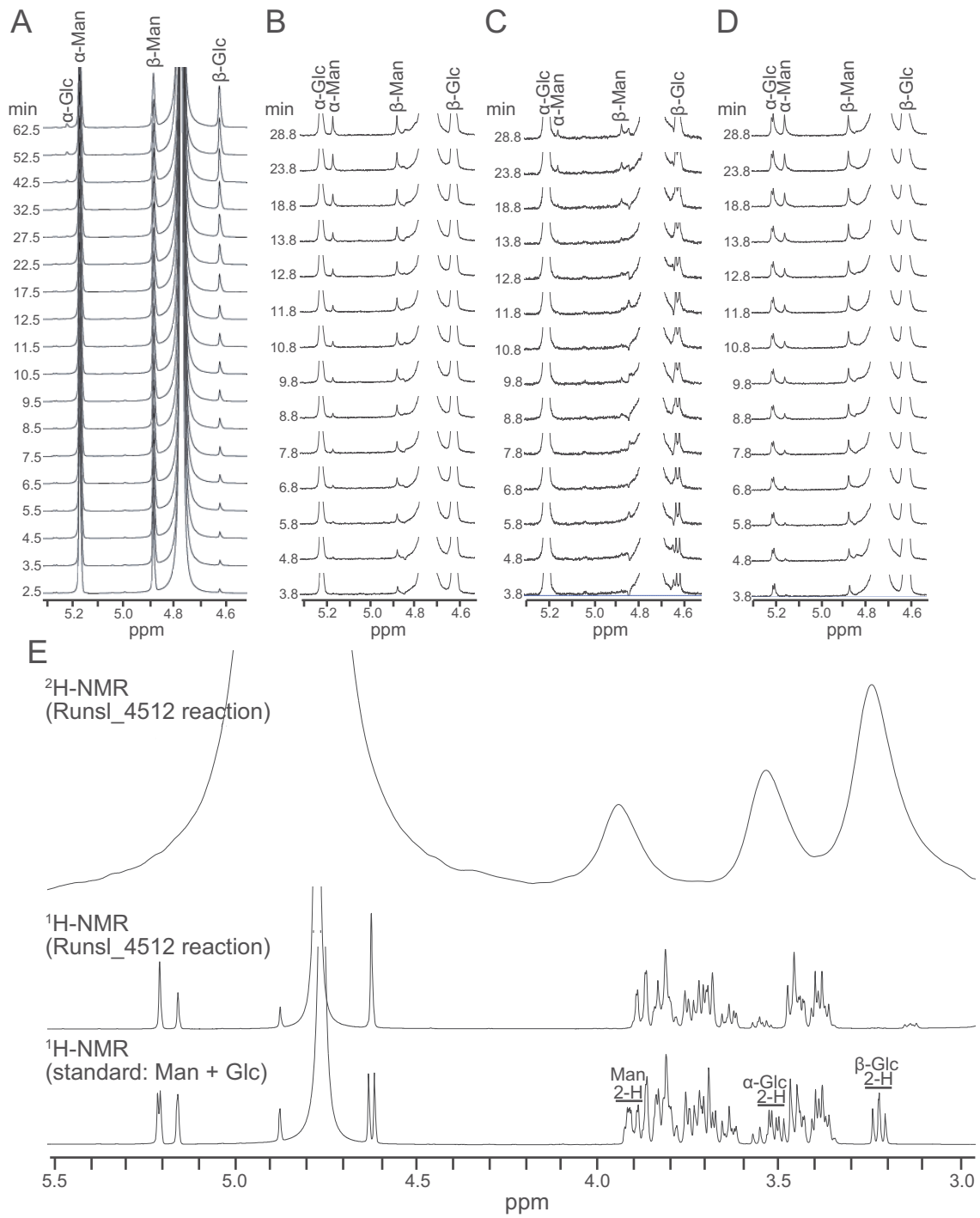Fig. 5., Saburi et al.

Fig. 6. Saburi et al.

α-helix 1                                                                        α-helix 2

```
Runsl_4512  -----MTSEKIASLRQEIETYLNTGLLPFWITRTVDKENGGFLTHFDQFGNDSGEDEKSLIAQSRSVFTYSSAHRAGYG  74
Dfer_5652   ------MNVDQLKSYREEIRQHLTSELLPFWENRAVDRENGGFITHFDNAGNDSGEDEKSLIAQTRTVYTFSSAHRAGYG  74
RaCE        -------------MMISEIRQELTDHIIPFWNK-LRDDENGGFYGYLSYGLGLDKKADKGVILHSRILWFYSNAYM-TLG  65
RmCE        MSTETIPDVRRLRALQAEVHEELTENILKFWATRTHDPVHGGFVGRVGPDGRPHPEAPRGAILNARILWTFAAAYR-QLG  79
MmMI        -------MSYPAFDSKTFLEAHIE-KTMAFYFPTCIDP-EGGFFQFFKDDGSVYDPNTRHLVSSTRFIFNFAQAYL-HTN  70
TfMI        ----MTLWTARAAHRAWLDAEAR-RLVDFAA--AADHPEHGF-AWLDGSGAPLPEQGVHTWITCRVTHVAALAHL--EG   69
EcSQI       ------MKWFNTLSHNRWLEQETD-RIFDFGK-NSVV--PTGF-GWLGNKGQIKEEMGTHLWITARMLHVYSVAAA--MG  67
AspAGE      -------MGKNLQALAQLYKNALLNDVLPFWENHSLDS-EGGYFTCLDRQGKVY-DTDKFIWLQNRQVWTFSMLCNQLEK  71
```

α-helix 3                                                              α-helix4              α-helix 5

```
Runsl_4512  GGVLAEMARHGVDYLINNMWDNEHGGFYWMTNRKGEVTIDQKIVYGLSFCIYSLSEYTLATGDPRGREYAEKTFDLLQKY  154
Dfer_5652   EGRYADIARHGVDFLINKMWDNEYGGFYWLMDRKGNVNIDEKIVYGHSFAIYSLAEYTLATGDPRGLEYAEKVFDLLQKH  154
RaCE        GDELLDNAKHAYEFIKNNCIDYEYGGVYWMMDFEGKPADTMKHTYNIAFAIYALSSYYRASGDKEALALAYRPFEDIEKN  145
RmCE        TPLYREMAERAYRYFVRHFVDAEHGGVYWMVAADGRPLDTRKHVYAQSFAIYALSEWHRATGGEAALALARSIYDLIETH  159
MmMI        IAEYKHAAVHGIQYLRQRH-QSQSGGYVWLLD-GGTNLDETNHCYGLAFVILAYSNALQ-IGLSEAEVWIEVTYDLLETH  147
TfMI        IPGASALADHGLRALAGPLRDPEHDGWFTALDSRGTVADSRKEAYQHAFVLLAAASATV-AGRPGARELLDAAAAVIEQR  148
EcSQI       RPGAYSLVDHGIKAMNGALRDKKYGGWYACVN-DEGVVDASKQGYQHFFALLGAASAVT-TGHPEARKLLDYTIEIIEKY  145
AspAGE      RENWLKIARNGAKFLAQHGRD-DEGNWYFALTRGGEPLVQPYNIFSDCFAAMAFSQYALASGEEWAKDVAMQAYNNVLRR  150
```

α-helix 6                      α-helix 7

```
Runsl_4512  AVDTHYGGYFEMFNRDWTLKG-----PGAAGGDRKTLDVHMHLMEAYTTLYECTGQ-EIHRRKLLETIELLVNKVMH-PE  227
Dfer_5652   GADTYYGGYFEMFHRNWDLKG-----PGAAGGDRKTLDAHMHLMEAFTTLYEASGK-QVHRRKLVEIIRLLINKIMH-PQ  227
RaCE        TLYEY--GYREAFDRQWRLV-DNEALSENGLKADKTMNAILHLIEAYTELYKADGN-EKVADRLKFQLGQMRDIVYT-PD  220
RmCE        CADRVHGGYVEACDRAWRPLEDARL-SAKDAPEPRSMNTHLHVLEAYANLYRVWPE-TELAARLQALIELFLRAIYH-PA  236
MmMI        FWENKHGLYLDEISSDWKTV-----------SPYRGQNANMHMCEALMSAFDATQN-PKYLDRAKLLAKNICQKQASLSN  215
TfMI        FWEEETGRCRESWDAAWHAD----------EPYRGANSNMHLVEAFLAAFDATGD-RVWAERALRIAHFFVHEVAR-PR  215
EcSQI       FWSEEEQMCLESWDEAFSKT----------EEYRGGNANMHAVEAFLIVYDVTHD-KKWLDRAIRVASVIIHDVAR-NN  212
AspAGE      -KDNPKGKYTKTYPGT-------------RPMKALAVPMILANLTLEM-EWLLPQETLENVLAATVQEVMGDFLD-QE  212
                                                       ▲
```

α7→α8 Loop                                        α-helix 8              α-helix 9

```
Runsl_4512  YGTGIPQFWADWSVAPQIKFDIVWGWDRFNPDGLKSAAEDNTSYGHNSEFAWLLMHALDILGL----PYDTYREQITKSY  303
Dfer_5652   YRTGIPQFWEDWSVAPQIKFDIIWGWDRFTEDGVKSSAEDNTSYGHNVEFAWLLMHALDIAGI----PYDEYHDQLKASY  303
RaCE        TNALKVFFDTAF----NLV------GD-------------IHSYGHDIEATWLMDRACDVLGD--EDLKKQFAEMDLKIS  275
RmCE        TGHLILFFDERW----RPR------SR----------AVSFGHDIEASWLLLEAVDVLGQ--ATLRPRVQQASLHLA  291
MmMI        SNEVWEHYTNDW----QID------WDYNKNDPKHLFRPWGFQPGHQTEWAKLLLMLDK-----RSPENWYLPKAKYLF  279
TfMI        DWRLPEHFTPDW----QVV------ADYNTDDRAHPFRPYGVTVGHVLEWARLLVHVEAAL----PDPPSWLLADAEAMF  281
EcSQI       HYRVNEHFDTQW----NPL------PDYNKDNPAHRFRAFGGTPGHWIEWGRLMLHIHAALEARCEQPPAWLLEDAKGLF  282
AspAGE      QGLMYENVAPDGSHIDCFE------GR------------LINPGHGIEAMWFIMDIARRKN------DSKTINQAVDVV  267
                                                                    ●
```

α-helix 10              α-helix 11

```
Runsl_4512  THAVENGVDW-EFGGVYVEGSHAG----QVYDKEKEFWQQAEMLIGMLDAYRFLKDEKYLQAYENIHRFVFDKMINHSL-  377
Dfer_5652   DHAVEYGIDW-EFGGVYVEGSHAG----EVYDREKEFWQQAEVIIGMLDAYRVYGDEKYLKAYDATHRFVFDKMIHHSV-  377
RaCE        HNIQDIALE--D-GALNNERD-KN-----EIDKTRVWWVQAEAVVGFINAYQHSGDEKFLESAKSVWENIKEYIIDKREG  346
RmCE        RATLAEGRA--PDGSLYYEIGEQG-----HLDTDRHWWPQAEALVGFLNAYQESGEVLFYEAAEDVWRYIRERQRDTRG-  363
MmMI        DLAYKKAWDT-KKGGLHYGYAPDG----TVCDPDKYFWVQAESFAAAWLLYKATKDETYYKQYLTLWEFSWNHMIDHTF-  353
TfMI        AAAVARGWSVDGTEGFVYTLDYDD----TPVVRSRMHWVVAEAISAAAVLGQRTGDERYEHWYRTWWDHAATYFVDTVQ-  356
EcSQI       NATVRDAWAPDGADGIVYTVDWEG----KPVVRERVRWPIVEAMGTAYSLYTVTGDRQYETWYQTWWEYCIKYLMDYEN-  357
AspAGE      LNILNFAWDN-EYGGLYYFMDAAGHPPQQLEWDQKLWWVHLESLVALAMGYRLTGRDACWAWYQKMHDYSWQHFADPEY-  345
```

α-helix 12

```
Runsl_4512  GEWWPLMTREGVPIW-K---HMSHSWKINYHDVRSMIQSIVRLDKIAKGV-----------             423
Dfer_5652   GEWLPLLTRQGEPIW-K---HMSHSWKVNYHSVRSMVQGIVRLNKLIGNK-----------             423
RaCE        GEWYSEVTFDHTPHDYK---ETVGPWKCPYHNGRMCMEVITRGVDI--------------             389
RmCE        GEWFARVRDDGAPYP-D---DKVDFWKGPYHNGRACLEAIQRLRHLLEHVRSR--------             412
MmMI        GAWYRILDENNAQYD-N---NKSPAGKTDYHTMGACYEVLKTLTL---------------             394
TfMI        GSWHHELDPTLAPPGGTWSGKP----DVYHAYQATRLPLLPLAPSLAGALATVG-----             407
EcSQI       GSWWQELDADNKVTT-KVWDGKQ----DIYHLLHCLVIPRIPLAPGMAPAVAAGLLDINAK             413
AspAGE      GEWFGYLNRRGEVLL-N---LKGGKWKGCFHVPRAMYLCWQQFEALS-------------             388
                                              ●
```
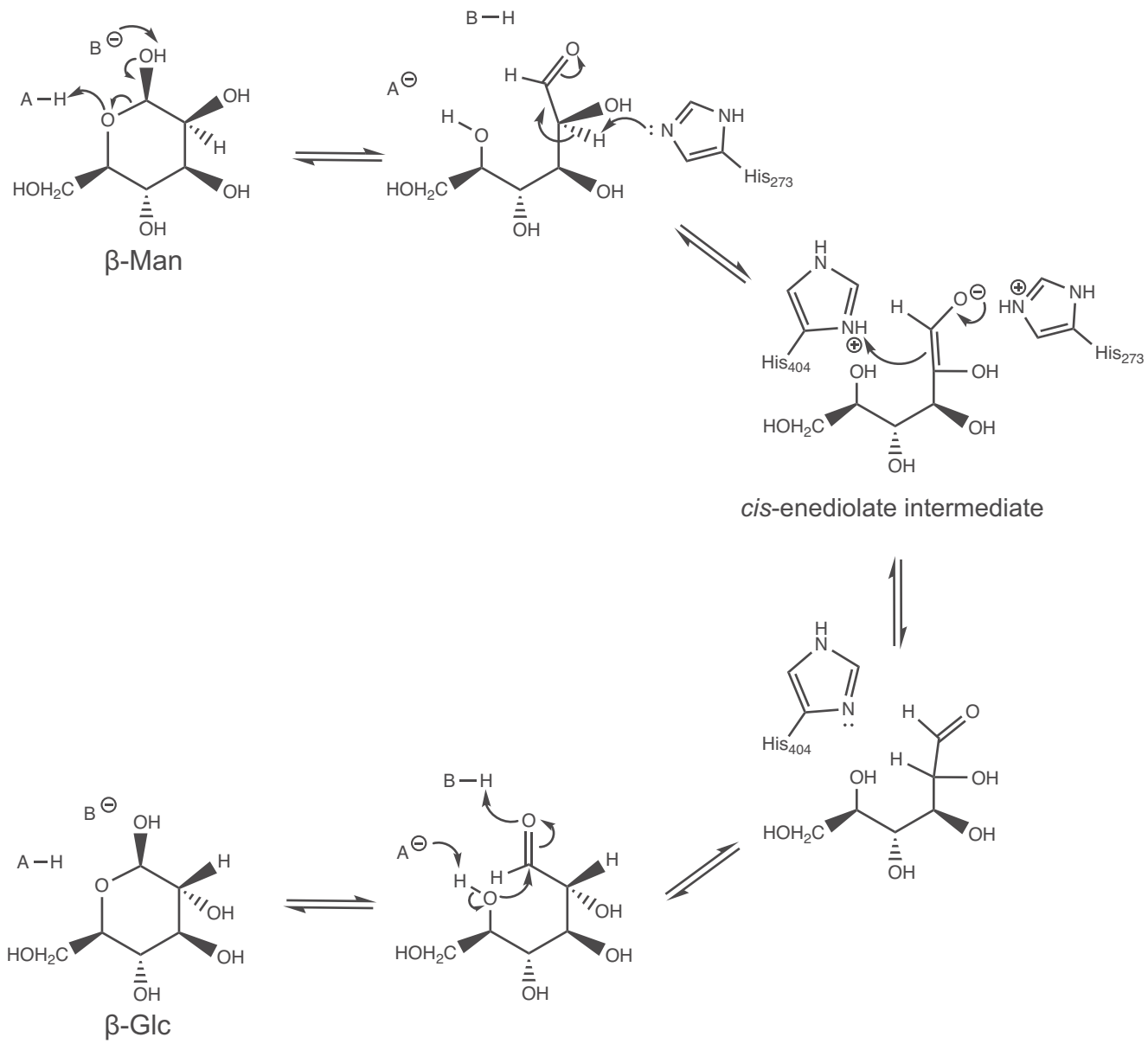
Fig. 7., Saburi et al.

β-Man

*cis*-enediolate intermediate

His273

His404

β-Glc

Fig. 8., Saburi et al.

Table 1. Sequences of primers used in this study.

| Name | Sequence (5′ to 3′) | Purpose |
| --- | --- | --- |
| Runsl_4512_s | TATATTTTT<u>CATATG</u>ACTTCTGAAAAAATT | Preparation of expression plasmid |
| Runsl_4512_a | AAATTATTC<u>CTCGAG</u>CACCCCTTTTGCAAT | Preparation of expression plasmid |
| Dfer_5652_s | CCATATTTT<u>GAATTC</u>ATGAATGTAGATCAA | Preparation of expression plasmid |
| Dfer_5652_a | TCCAAATTC<u>CTCGAG</u>CTTATTTCCAATCAG | Preparation of expression plasmid |
| D187N_s | ACCCTC**AAT**GTACACATGCACCTCATG | Mutagenesis in Runsl_4512 |
| D187N_a | GTGTAC**ATT**GAGGGTCTTGCGGTCACC | Mutagenesis in Runsl_4512 |

Recognition sites of restriction endonucleases are underlined. Substituted nucleotides are shown in bold face.

Table 2. Kinetic parameters of Runsl_4512 and Dfer_5652 for D-mannose.

| Enzyme | $k_{cat}$ (min$^{-1}$) | $K_m$ (mM) | $k_{cat}$/ $K_m$ (min$^{-1}$ mM$^{-1}$) |
|---|---|---|---|
| Runsl_4512 | 286 ± 20 | 73.5 ± 6.7 | 3.89 |
| Dfer_5652 | 233 ± 25 | 66.4 ± 11.1 | 3.51 |
| CsCE | 44.3 ± 0.6 | 51.8 ± 1.2 | 0.855 |
| CvCE | 6.78 ± 0.18 | 245 ± 10 | 0.0277 |

Values are mean ± standard deviation for three independent experiments. CsCE, *Caldicellulosiruptor saccharolyticus* CE (Park et al. 2011); CvCE, *Cellvibrio vulgaris* CE (Saburi et al. 2015).